Journal of Building Engineering 28 (2020) 101059

Contents lists available at ScienceDirect

Journal of Building Engineering

journal homepage: http://www.elsevier.com/locate/jobe

Walls comparative evaluation for the thermal performance improvement of low-rise residential buildings in warm Mediterranean climate

Paolo Maria Congedo, Cristina Baglivo *, Giulia Centonze

Department of Engineering for Innovation, University of Salento, 73100, Lecce, Italy

ARTICLE INFO

Keywords:
Envelope
Optimization
Operative air temperature
Warm climate
Ventilation

ABSTRACT

Buildings built in warm climates are affected by severe overheating problems in summer, which negatively affects people's comfort and health. For these reasons, many users are forced to install cooling systems, leading to an increase in costs, consumption and a meaning impact on the environment.

This study gives a valid method to monitor the overheating problems in buildings located in Mediterranean climates, without the use of cooling systems, but just with an accurate design of the envelope. The main challenge is to demonstrate that the hourly monitoring of the internal operative temperature (TOP), in accordance with the UNI EN ISO 52016, is able of defining univocally the performances of the building, taking into consideration the characteristics of the envelope. The optimization of this parameter permits to reach high level of internal comfort in a building, ensuring the designer to identify the best choice of building materials that compose the envelope.

The TOP trends, for a whole year, are tested on a single-residential building model located in a warm Mediterranean climate, considering different configurations of the external walls.

The results put in evidence that the best solutions are characterized by the presence of the double layer of tuff, with a very massive layer in the internal side and resistive layer outside.

At the end, this study demonstrates that once optimized the envelope, it is easier to reach good values of internal operative temperature with the only use of a mechanical ventilation system.

1. Introduction

The reduction of the energy consumption in buildings is a topic of great attention at European level. It is estimated that building stock accounts for about 36% of greenhouse gas emissions [1]. The European polices aim to promote the growth of a sustainable, competitive, safe and decarbonized energy system.

The goal of several studies [2,3] is to identify the best compromise between energy consumption and economic feasibility, for example Valdiserri et al. [4] show retrofitting actions and economic evaluation of an existing office building.

Another important aspect addressed in the literature is the impact on the environment of the construction life cycle, with the consequent identification of strategies to reduce CO_2 emissions, guaranteeing a high level of internal comfort [5–7]. It is proved that an accurate maintenance scheduling of the building leads to an energy saving and a reduction of CO_2 emissions [8]. The study [9] analyses how the design strategies can affect the energy consumption, also considering the shape of the building.

The International Energy Agency (IEA) [10] has identified six parameters that affect the building energy consumption: climate, building envelope, energy systems and services, interior design criteria, operation and maintenance of buildings, behavior of the occupants. Many of these parameters have been extensively analyzed in the literature.

Overheating within buildings causes adverse effects on the health and well-being of the population, it is very important to identify a set of sustainable and practical solutions to this problem. Very isolated buildings with several air cavities, buildings with no good ventilation and excessive heat gains are affected by overheating problems [11]. Studies [12–14] have been carried out on walls, windows and technical systems, to show that combinations with high masses are the best solutions in terms of internal comfort and costs for the hot climate. The position of the insulation layer on external walls is investigated by Ref. [15], considering the dynamic transfer and the effect of relative humidity. The results put in evidence how the internal relative humidity significantly influences the heat transfer process. The study [16]

* Corresponding author.
E-mail address: cristina.baglivo@unisalento.it (C. Baglivo).

https://doi.org/10.1016/j.jobe.2019.101059
Received 24 May 2019; Received in revised form 5 September 2019; Accepted 6 November 2019
Available online 8 November 2019
2352-7102/

confirms, with numerically analyses, that the energy used for heating and cooling a room in Shanghai is highly reduced by the addition of insulating layers on the external side of the wall, compared to configurations with internal insulation.

This study has been carried out in order to identify a simple index to represent the thermal performance of the building envelope, during the whole year in a Mediterranean climate. To reach this goal several wall configurations with different thermal characteristics, representing the most used in the Italian context, are analyzed.

1.1. The importance of the ventilation in building

The ever more restrictive building regulations on energy efficiency have led, in the field of new buildings, to the construction of buildings with low energy consumption. The use of new materials for construction and insulation ensures an airtightness of the buildings, which however no longer guarantees the minimum air exchange of the rooms. To ensure health and well-being, but also to eliminate harmful substances in construction materials, enough air exchange is absolutely necessary in the home. A controlled mechanical ventilation system is the ideal solution, providing the necessary air exchange and regulating the level of humidity in the rooms, it prevents the formation of mold. This ensures an always optimal air quality, in fact, with a VMC (controlled mechanical ventilation system), it is possible to have constant controlled renewal of air in all environments.

The study [17] puts in evidence that natural night-time ventilation could save cooling energy in office buildings, while the use of mechanical ventilation could lead to greater energy consumption.

The benefits obtainable by a night-time ventilation for residential case have been studied by Ref. [18], considering the hot and humid climate of Malaysia. Starting from a survey, the study shows that most users prefer daytime ventilation rather than night ventilation.

The study [19] puts in evidence the importance to use the thermal mass and night ventilation for the reduction of the maximum peak of internal temperature during the summer period, considering different hot humid climate locations in Israel.

Many studies show that natural ventilation improves thermal comfort and indoor air quality and energy savings. The paper [20] shows how thermal comfort is influenced by architectural and structural design features, window orientation, shading and microclimate.

The efficacy of cooling ventilation for residential building is also confirmed by Ref. [21]. The results show that night-time ventilation is the most effective strategy for passive cooling.

1.2. The impact of the climate on the building performances

The climate strongly affects the internal comfort of the buildings. A design focused on reducing energy consumption and improving living comfort, capable of exploiting local natural resources and the climate, is generally based on a bioclimatic approach.

Nowadays there are many innovative and efficient solutions that aim to reduce energy consumption. Careful design of the building is the basis in the control of the exchanges between internal and external spaces [22]. As aforementioned, if there is no proper internal ventilation, the air quality can be poor, even when the building has high efficiency walls and windows [23].

Harkouss et al. [24] presented a multi-objective analysis for the passive design optimization of low energy buildings for several climates, using the twenty-five different climates of Köppen-Geiger classification [25].

Other studies focus on the building envelope putting in evidence strategies to obtain high efficiency envelope for building in cold climate [26] and warm climate [27].

In composite climates [28], walls with high thermal mass values ensure comfort in both summer and winter. In cold climates [29], it is possible to use multi-layer walls with high thickness and low-density thermal insulation to reach very low constant thermal transmittance.

In warm climate [30], to avoid the overheating in summer season, it is important to design external walls with low values of decrement factor, high values of internal areal capacity and time shift. It is essential to evaluate the size of the windows and the presence of thermal break. Today the films and coatings represent a valid support to limit solar gains. Low solar gain glasses reduce electricity requirements [31].

The behavior of windows is influenced by different climates; low solar gain windows are suitable in hot climates, while high solar gain windows are preferred for cold climates.

The study proposed by Ref. [32] focuses on the limit to the effect of overheating in buildings located in hot climates. It demonstrated that the shading systems and the presence of overhangs are fundamental in controlling the entry of solar radiation and therefore avoid the overheating during the summer.

A Mediterranean climate is chosen for simulations of this study. The climatic classification of Italian municipalities was introduced to regulate the period of operation of the heating systems with the purpose of limiting energy consumption. Lecce belongs to climate zone C, assigned by Decree of the President of the Republic n. 412 of 26 August 1993. In accordance with the Köppen-Geiger classification, city of Lecce is classified as Csa characterized by a hot Mediterranean/dry-summer subtropical climate.

1.3. Comfort assessment and thermal behavior

The thermal comfort refers to the satisfaction of the thermal environment expressed by the users. The widely used comfort indexes are PPD (expected percentage of dissatisfied) and PMV (average expected score) [33]. The model, adopted by the American Society of Heating and Air-Conditioning Engineers (ASHRAE), permit to predict the percentage of dissatisfied people due to the draft depending on the average air speed, the intensity of the turbulence and the air temperature, starting from several parameters, such as the building size and geometry, airflows rates and temperatures, relative humidity, mean radiant temperature, air velocity, and heat sources. Results are also influenced by the people metabolic rate and clothing insulation [34]. The sense of comfort is reached for PMV values of-0.5 and + 0.5, meaning that 90% of people are satisfied. Pourshaghaghy et al. [35] evaluated the air conditioning system considering the thermal comfort with the PMV and PPD indexes, in accordance with ISO-7730 [36].

Other studies [37–39] demonstrate that a comfortable internal microclimate guarantee human health, improving also the workplace productivity. Seppänen et al. [40,41] show that if there is a decrease in productivity in indoor environments by 2%, the air temperature increases in a range of 25–32 °C.

This study proposes the internal operative temperature (TOP), as a simple index to represent the thermal performance of the building envelope, during the whole year. The operative temperature (TOP) is defined as a simplified measure of human thermal comfort; derives from the average radiant temperature and internal air temperature, according to ASHRAE and ISO standards. It is the uniform temperature of the air and walls of the specific environment [42].

The TOP is also useful in assessing and improving the thermal comfort level of the occupants: mathematically, it can be expressed as

$$TOP = (h_r T_{mr} + h_c T_{db})/(h_r + h_c) \quad (1)$$

where.

T_{mr} = mean radiant temperature
h_r = linear radiative heat transfer coefficient
T_{db} = air (dry bulb) temperature
h_c = convective heat transfer coefficient

2. Methodology

The objective of the study is the analysis of different envelope configurations to achieve an optimal standard for the considered climate, using the internal operative air temperature like quality indicator.

2.1. Description of the case study building

The reference buildings are representative of a typical and average housing stock in a given Member State. The most common type is a small building, though the type of Italian construction is heterogeneous. Single-residential buildings make up about 60% while multi-apartments account for about 39% of the national building stock [43]. The rate of new construction is around 2% for year.

The study has been focused on a mono residential building, suitable for a single family composed by four people. The geometry is simple and compact (S/V = 0.67), composed by a deposit and two floors, as reported in Fig. 1. The tridimensional model is shown in Fig. 2.

The first floor is used as living area, with kitchen, living room, bathroom and utility room, while the second floor is used as sleeping area with two bedrooms, bathroom and utility room. The internal height of each floor is 2.7 m.

The HVAC system is not considered in order to identify the best envelope solution without the use of air conditioning system.

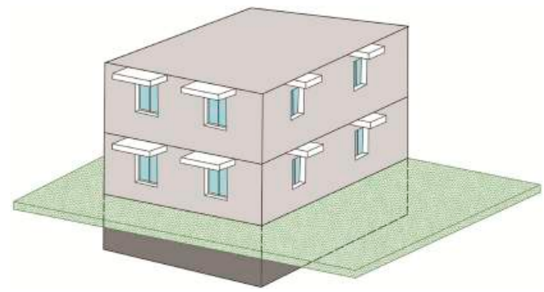

Fig. 2. The case study, tridimensional model.

2.1.1. The building envelope

The design of a good building envelope is the first element in reducing the thermal loads. Table 1 presents the characteristics of all building materials, in terms of thickness, thermal conductivity, specific heat and density. Table 2 shows the layers of the internal partition walls (wt).

Table 3 shows the layers of the opaque horizontal partitions: F1 is the floor between internal environments, F2 from the interior to the

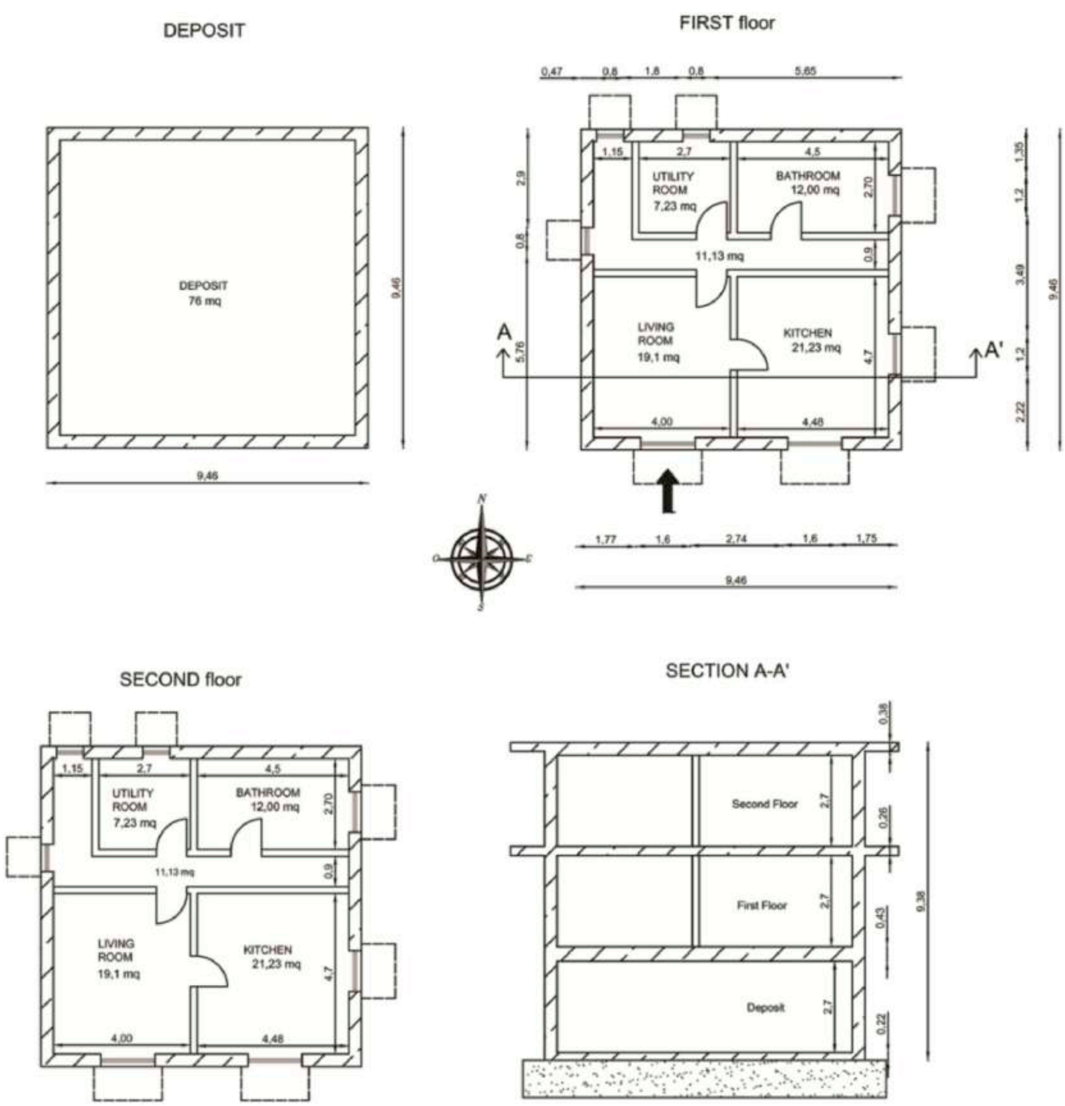

Fig. 1. The case study.

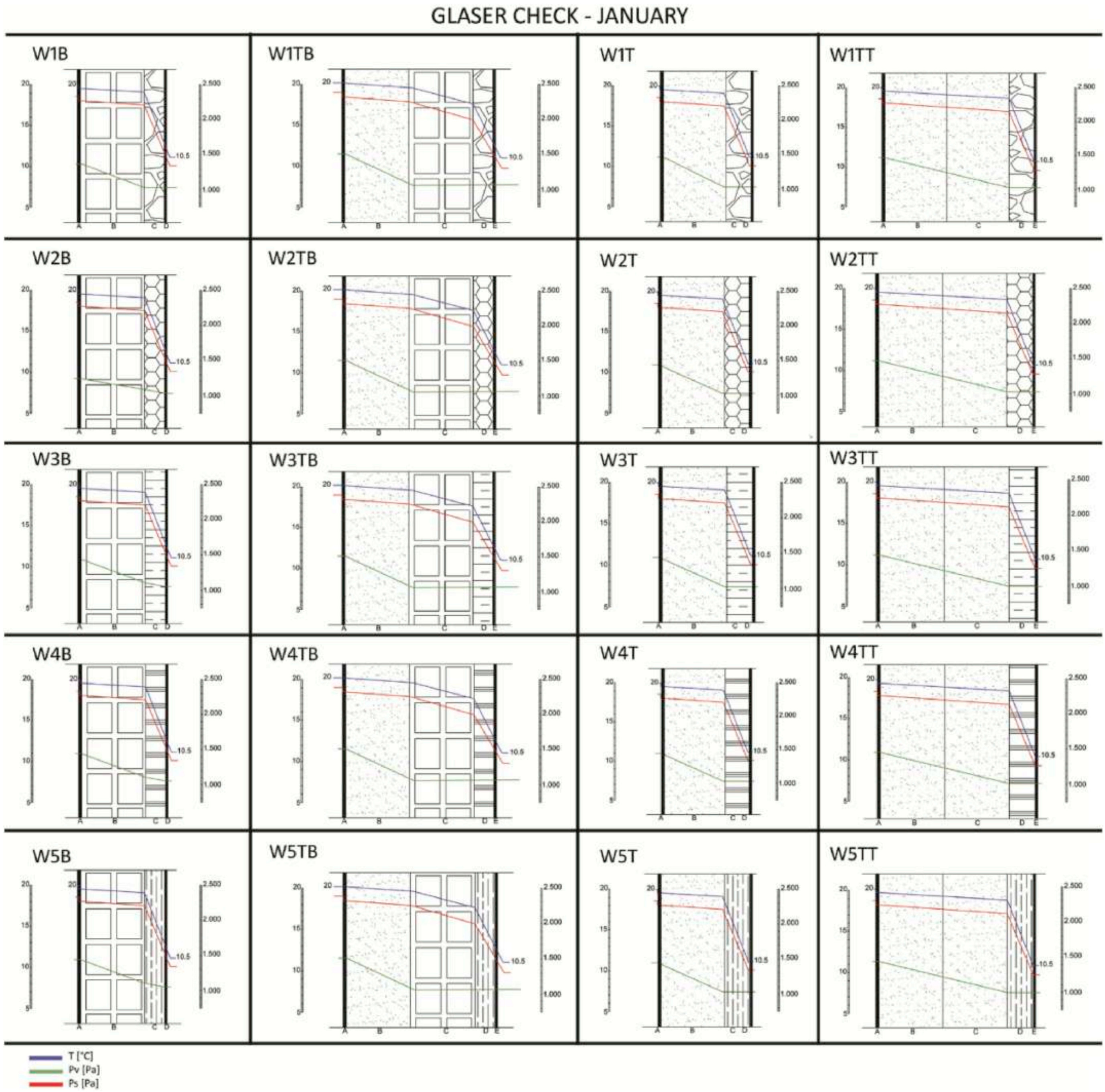

Fig. 3. Thermo-hygrometric check.

unheated area, F3 from unheated area to the ground, R1 is the roof of the building.

The windows can make a high contribution to the energy efficiency of a building during its useful life [44]. Windows have optical and thermal properties that make them more "vulnerable" to energy losses than opaque construction elements [45]. The cooling performance of windows for residential buildings, constructed in a warm climate, must be taken into consideration.

Table 4 presents the thermal characteristics of windows, characterized by double glass 4-15-4 with argon inside and pvc frame with thermal break. All windows have closings darkening and screenings in aluminum blinds with high permeability.

The assessment of the dynamic thermal performance of the envelope has been calculated in accordance with the procedure defined by the European norm EN ISO 13786 [46].

The thermal values are the results of the imposed conductive thermal exchange condition applied to the envelope. A sinusoidal function of time describes the temperature and heat flow rate, a period of 86400 s, which corresponds to daily meteorological variations and temperature setback, is considered.

Thermal conductivity, specific heat, density and thickness of all building materials, of which the walls are composed, are necessary for the calculation of the dynamic thermal parameters.

The heat transfer matrix Z correlates the complex amplitude of temperature and heat flow rate at the external side to the internal one. The calculation of the periodic penetration depth δ, in function of the building material properties, and ξ, relatives to the ratio of the thickness of the layer to δ, are necessary to determine the values of the heat

Table 1
Thermal characteristics of building materials.

Materials	Thickness (mm)	λ (W/mK)	c (J/KgK)	ρ (kg/m^3)
Bricks	80	0.364	1	1800
Tuff	180–250	1.7	1.3	2300
Wood fiber panels flexible	80–100	0.038	2.1	49.5
Expanded cork panels	80–100	0.038	1.9	120
Hemp fibers	80-100-120	0.03	2.2	38
Expanded polyurethane	80–90	0.023	1.255	36
Expanded polystyrene	80–100	0.034	1.7	35
Exterior and interior plaster	10	0.9	0.84	1800
Ceramic tiles	10	1.3	0.84	2300
Slab in brick blocks and CLS joists	240	0.686	1	900
Lightweight concrete screed	60	1.08	1	1600
Rock wool	50–100	0.038	1.03	150
Bitumen	3	0.17	0.92	1200
Vapor barrier	5	0.4	1.5	360
Bituminous waterproofing membrane	3	0.17	1	1200
Tile roof	20	0.825	0.84	1800
Reinforced concrete	60	1.91	1	2400

transfer matrix Z.

$$\delta = \sqrt{\frac{\lambda T}{\pi \rho c}} \tag{2}$$

Table 4
Thermal characteristics of windows.

n.	Geometry (mm)	Ug (W/m^{2}K)	Uf (W/m^{2}K)	Uw (W/m^{2}K)
f11	80x150	1.522	2.2	2.360
f12	120x150			2.148
f13	160x150			2.042

$$\xi = \frac{d}{\delta} \tag{3}$$

Thermal admittance is a complex quantity resulting from the complex amplitude of heat flow density across the surface of the component, divided by the complex temperature amplitude in the same area when the temperature on the other side is kept constant.

Decrement factor is the ratio of the modulus of the periodic thermal transmittance to the steady-state thermal transmittance U.

Time shift is a period between the maximum amplitude of a cause and the maximum amplitude of its effect.

Areal heat capacity is the heat capacity divided by area of element, to prevent the occurrence of overheating phenomena, it is important to have a high internal areal heat capacity, as it is directly related to the heat storage capacity of the wall.

Table 5 reports the external walls variants with their main physical characteristics and the composition of the different layers of which they are made of.

Table 2
Thermal characteristics of partition wall.

n.	Layers	d (mm)	U (W/m^{2}K)	Δt (h)	fd	k_1 (kJ/m^{2}K)	k_2 (kJ/m^{2}K)	Y_{11} (W/m^{2}K)	Y_{22} (W/m^{2}K)	Y_{12} (W/m^{2}K)	Ms (Kg/m^2)
wt	Lime and cement plaster 10 mm Tuff 180 mm Lime and cement plaster 10 mm	200	3.284	6.31	0.4067	83.940	158.260	5.5100	10.76	1.340	414

Table 3
Thermal characteristics of opaque horizontal partitions.

n.	Layers	d (mm)	U (W/m^{2}K)	Δt (h)	f_d	k_1 (kJ/m^{2}K)	k_2 (kJ/m^{2}K)	Y_{11} (W/m^{2}K)	Y_{22} (W/m^{2}K)	Y_{12} (W/m^{2}K)	M_s (Kg/m^2)
F1 (between interior environments)	Ceramic tiles 10 mm Slab in brick blocks and CLS joists 240 mm Lime and cement plaster 10 mm	260	1.718	6.15	0.540	56.690	87.870	3.61	5.73	0.930	239
F2 (from inside to unheated area)	Ceramic tiles 10 mm Lightweight concrete screed 60 mm Rock wool 100 mm Vapor barrier 5 mm Slab in brick blocks and CLS joists 240 mm Lime and cement plaster 10 mm	425	0.293	14.2	0.098	60.553	48.319	4.39	3.50	0.030	352
F3 (from unheated area to the ground)	Ceramic tiles 10 mm Reinforced concrete 60 mm Extruded polystyrene panel 50 mm Concrete 60 mm Coarse gravel without clay 40 mm	220	0.637	7.55	0.334	68.390	133.390	4.80	9.50	0.210	369
R1 (from internal to external)	Lime and cement plaster 10 mm Slab in brick blocks and CLS joists 240 mm bitum 3 mm Rock wool 50 mm Bituminous waterproofing membrane 3 mm Tile roof 20 mm	376	0.31	10.37	0.204	56.135	38.511	4.02	2.76	0.060	274

Table 5
Thermal characteristics of external walls.

n.	Layers (from internal to external side)	d (mm)	U (W/m^{2}K)	Δt (h)	fd	k_1 (kJ/m^{2}K)	k_2 (kJ/m^{2}K)	Y_{11} (W/m^{2}K)	Y_{22} (W/m^{2}K)	Y_{12} (W/m^{2}K)	M_s (Kg/m^2)
W1B	Lime and cement plaster 10 mm Brick 250 mm Wood fiber panels flexible 80 mm Lime and cement plaster 10 mm	350	0.335	15.31	0.047	56.380	18.820	4.090	1.370	0.020	454
W1TB	Lime and cement plaster 10 mm Tuff 250 mm Brick 250 mm Wood fiber panels flexible 80 mm Lime and cement plaster 10 mm	600	0.319	23.45	0.005	77.022	18.918	5.6029	1.38	0.000	1.029
W2B	Lime and cement plaster 10 mm Brick 250 mm Expanded cork panels 80 mm Lime and cement plaster 10 mm	350	0.335	16.33	0.045	56.330	21.820	4.0900	1.59	0.010	460
W2TB	Lime and cement plaster 10 mm Tuff 250 mm Brick 250 mm Expanded cork panels 80 mm Lime and cement plaster 10 mm	600	0.319	24.47	0.005	77.025	21.961	5.6029	1.60	0.000	1.035
W3B	Lime and cement plaster 10 mm Brick 250 mm Hemp fibers 80 mm Lime and cement plaster 10 mm	350	0.282	15.32	0.045	56.370	17.870	4.0970	1.31	0.010	453
W3TB	Lime and cement plaster 10 mm Tuff 250 mm Brick 250 mm Hemp fibers 80 mm Lime and cement plaster 10 mm	600	0.271	23.46	0.005	77.027	17.697	5.6028	1.31	0.000	1.028
W4B	Lime and cement plaster 10 mm Brick 250 mm Expanded Polyurethane 80 mm Lime and cement plaster 10 mm	350	0.229	15.17	0.044	56.370	16.590	4.0969	1.21	0.010	453
W4TB	Lime and cement plaster 10 mm Tuff 250 mm Brick 250 mm Expanded Polyurethane 80 mm Lime and cement plaster 10 mm	600	0.222	23.31	0.005	77.030	16.665	5.6028	1.21	0.000	1.028
W5B	Lime and cement plaster 10 mm Brick 250 mm Expanded Polystyrene 80 mm Lime and cement plaster 10 mm	350	0.309	15.12	0.047	56.397	17.469	4.0969	1.27	0.010	453
W5TB	Lime and cement plaster 10 mm Tuff 250 mm Brick 250 mm Expanded Polystyrene 80 mm Lime and cement plaster 10 mm	600	0.296	23.26	0.005	77.024	17.545	5.6029	1.28	0.000	1.028
W1T	Lime and cement plaster 10 mm Tuff 250 mm Wood fiber panels flexible 100 mm Lime and cement plaster 10 mm	370	0.337	11.28	0.079	77.440	19.190	5.600	1.380	0.030	580
W1TT	Lime and cement plaster 10 mm Tuff 250 mm Tuff 250 mm Wood fiber panels flexible 100 mm Lime and cement plaster 10 mm	620	0.321	19.07	0.011	77.012	18.972	5.6022	1.38	0.000	1.155
W2T	Lime and cement plaster 10 mm Tuff 250 mm Expanded cork panels 100 mm Lime and cement plaster 10 mm	370	0.337	12.57	0.072	77.360	22.550	5.6000	1.63	0.020	587
W2TT	Lime and cement plaster 10 mm Tuff 250 mm Tuff 250 mm Expanded cork panels 100 mm Lime and cement plaster 10 mm	620	0.321	20.36	0.01	77.000	22.467	5.6022	1.64	0.000	1.162
W3T	Lime and cement plaster 10 mm Tuff 250 mm Hemp fibers 100 mm Lime and cement plaster 10 mm	370	0.272	11.29	0.078	77.360	18.250	5.6000	1.32	0.020	579
W3TT	Lime and cement plaster 10 mm Tuff 250 mm Tuff 250 mm Hemp fibers 100 mm Lime and cement plaster 10 mm	620	0.262	19.08	0.011	77.017	18.092	5.6022	1.31	0.000	1.154
W4T	Lime and cement plaster 10 mm	360	0.235	10.55	0.079	77.330	16.795	5.6051	1.21	0.020	578

(continued on next page)

Table 5 (*continued*)

n.	Layers (from internal to external side)	d (mm)	U (W/m^2K)	Δt (h)	fd	k_1 (kJ/m^2K)	k_2 (kJ/m^2K)	Y_{11} (W/m^2K)	Y_{22} (W/m^2K)	Y_{12} (W/m^2K)	M_s (Kg/m^2)
	Tuff 250 mm Expanded Polyurethane 90 mm Lime and cement plaster 10 mm										
W4TT	Lime and cement plaster 10 mm Tuff 250 mm Tuff 250 mm Expanded Polyurethane 90 mm Lime and cement plaster 10 mm	610	0.227	18.34	0.011	77.024	16.626	5.6022	1.21	0.000	1.153
W5T	Lime and cement plaster 10 mm Tuff 250 mm Expanded Polystyrene 100 mm Lime and cement plaster 10 mm	370	0.305	10.59	0.08	77.413	17.685	5.6053	1.27	0.020	579
W5TT	Lime and cement plaster 10 mm Tuff 250 mm Tuff 250 mm Expanded Polystyrene 100 mm Lime and cement plaster 10 mm	620	0.292	18.38	0.011	77.019	17.452	5.6022	1.27	0.000	1.154

The walls from 1 to 5 have different insulation layers, such as wood fiber panels flexible (W1), expanded cork panels (W2), hemp fibers (W3), expanded polyurethane (W4) and expanded polystyrene(W5). These insulation materials are the most used in the Italian building sector. The thicknesses of the insulating materials of the configurations vary according to the transmittance value obtained. The walls are designed to meet Italian transmittance limits, related to climate zone C, to which the case study belongs. Furthermore, insulating materials have different thermal characteristics and the choice involves having both natural and synthetic materials, allowing the choice of highly sustainable and technically advantageous solutions.

Considering that a large part of walls in the Italian context are realized in brick or in tuff, as massive layer, this study puts in evidence the performances of the walls with these materials. In fact, first each typology of wall (W1, W2, W3, W4 and W5) is coupled with a single layer of brick (W1B, W2B, W3B, W4B and W5B) and with a layer of brick and a layer of tuff (W1TB, W2TB, W3TB, W4TB and W5TB). Secondly, each typology of wall is coupled with a single layer of tuff (W1T, W2T, W3T, W4T and W5T) and with a double layer of tuff (W1TT, W2TT, W3TT, W4TT and W5TT).

The TOP is tested considering all walls for the first (FF) and second floor (SF) of the building, for a total of 40 combinations.

This analysis permits the designer to address measures on the walls, preferring the choice of insulating materials or the addition of a massive layer.

Fig. 3 shows the Hygrothermal performance test (Glaser) for all wall configurations.

The calculation has been carried out in agreement with the norm EN ISO 13788 [47], the analysis is analytical and monthly. The evaluation is done considering the temperature data of Lecce (Italy) and the check is shown for January, the critical month of the wintertime of the considered climate. The aim is to monitor the surface and interstitial condensation, to avoid the mold risk.

The method allows, once the internal and external thermo-hygrometric conditions have been set, to verify whether vapor condensation may occur in a supposedly initially dry flat structure.

The distribution of temperature of all the interface layers (Tn), which compose the wall, is calculated with the following equation:

$$Tn = Te + \frac{Rn}{Rtot}\ (Ti - Te) \tag{4}$$

Where:

- Te is the external temperature [°C];
- Ti is the internal temperature [°C];
- Rn is the thermal resistence [m^2K/W];
- Rtot is the total resistence [m^2K/W];

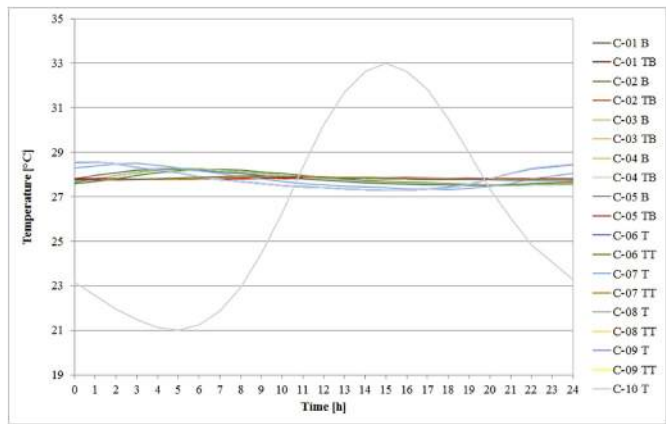

Fig. 4. Trend of the internal surface temperatures of all external walls compared with external temperature.

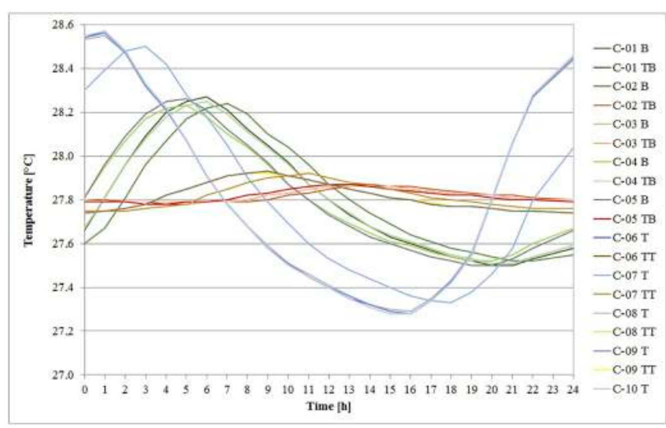

Fig. 5. Trend of the internal surface temperatures of all external walls.

The Glaser diagram represents the trend of the temperature values within the structure with the relative values of the saturation vapor pressure (Ps); comparing the latter with the values of partial vapor pressures (Pv), the possibility of condensation risks is established. The formation of condensation in a wall layer can therefore be easily deduced when the partial pressure value is greater than that of the saturation pressure.

From the Glaser check, reported in Fig. 3, it is evident that all the analyzed walls do not shows the risk of condensation in January.

The internal surface temperatures of the wall combinations and the external temperature are represented in Fig. 4, the internal surface ones in details in Fig. 5.

In particular, there are the Combinations from C-01 B to C 05 B, characterized by the presence of a single brick layer, by varying the insulant material; the combinations from C-01 TB to C-05 TB, characterized by a double layer (tuff-brick); the Combinations from C-06 T to C 10 T, characterized by the presence of a single layer in tuff; the combinations from C-06 TT A C-10 TT, characterized by a double layer (tuff-tuff). It is noted that there is a Δt until more than 4 °C between the external temperature and the internal surface temperature trends. It is interesting to underline the small oscillation of the internal surface temperatures.

The combinations C-01 B - C 05 B and C-06 T - C 10 T are those with the maximum oscillations. For the combinations C-01 B - C 05 B, there is a peak of 28.3 °C up to a minimum peak of 27.5 °C. For the combinations C-06 T - C 10 T, there is a peak value of 28.6 °C up to a minimum peak of 27, 4 °C.

Besides, for the combinations C-01 TB - C 05 TB and C-06 TT - C 10 TT, a double layer has been added, respectively, of bricks and tuff. The curves are very flat, the maximum peak is 27.85 °C, showing the best behavior in terms low variation of internal surface temperature.

2.2. The calculation tools

Termolog Epix 9 [48] is the software used for the calculation of the hourly energy performance of the building, by the Dynamic Calculation Engine. The algorithms are based on the hourly method proposed by the UNI EN ISO 52016 [49] in accordance with ASHRAE 140–2017 [50]. The hourly method allows the assessment of the internal temperature of a thermal zone by resolution, in a transitory regime on an hourly basis, of a system of equations which describe the thermal exchanges that occur between internal and external environment through the envelope. The equations are solved in matrix form. Each building component (floor, window, wall) is modeled in a series of nodes (capacity and thermal resistances). This method permits to calculate the hourly energy balance of the building envelope and allows to obtain the trend of the internal temperatures (operating temperature, radiant temperature and air temperature) and the required thermal load of the system. In particular, the standard provides the following assumptions:

- the air temperature is considered uniform throughout the thermal zone;
- the surfaces of each element of the envelope are isothermal;
- the conduction of heat through the elements of the room or area (excluding towards the ground) is assumed as one-dimensional;
- the heat storage capacity of thermal bridges is neglected;
- the thermal bridges are directly thermally coupled to indoor and outdoor air temperatures;
- the air cavities of the envelope are treated as air layers delimited by two isothermal and parallel surfaces;
- the thermophysical properties of the materials are independent of time, but variations in the properties of the components are not excluded: such as mobile solar blinds, shutters;
- the external radiant environment (excluding the sky) is at the temperature of the outside air;
- the spatial distribution of solar radiation within the room is uniform and independent of time;
- the average radiant temperature is calculated as weighted average of internal surface temperatures multiplied by the area of each component.

Table 6
List of combinations.

Combo	Walls	Combo	Walls
C-01 FF-B	W1B	C-06 FF-T	W1T
C-01 SF-B	W1B	C-06 SF-T	W1T
C-01 FF-TB	W1TB	C-06 FF-TT	W1TT
C-01 SF-TB	W1TB	C-06 SF-TT	W1TT
C-02 FF-B	W2B	C-07 FF-T	W2T
C-02 SF-B	W2B	C-07 SF-T	W2T
C-02 FF-TB	W2TB	C-07 FF-TT	W2TT
C-02 SF-TB	W2TB	C-07 SF-TT	W2TT
C-03 FF-B	W3B	C-08 FF-T	W3T
C-03 SF-B	W3B	C-08 SF-T	W3T
C-03 FF-TB	W3TB	C-08 FF-TT	W3TT
C-03 SF-TB	W3TB	C-08 SF-TT	W3TT
C-04 FF-B	W4B	C-09 FF-T	W4T
C-04 SF-B	W4B	C-09 SF-T	W4T
C-04 FF-TB	W4TB	C-09 FF-TT	W4TT
C-04 SF-TB	W4TB	C-09 SF-TT	W4TT
C-05 FF-B	W5B	C-10 FF-T	W5T
C-05 SF-B	W5B	C-10 SF-T	W5T
C-05 FF-TB	W5TB	C-10 FF-TT	W5TT
C-05 SF-TB	W5TB	C-10 SF-TT	W5TT

- the convective heat transfer coefficients on the external surface depend on the wind speed and direction, but are considered time-invariant;
- the convective heat transfer coefficients on the inner surface depend on the direction of the heat flow but are considered time-invariant.

3. Results and discussions

The list of combinations analyzed is reported in Table 6. All walls presented are applied on the first (FF) and second floor (SF).

3.1. Operative temperature evaluation

The first analysis has been conducted with both the cooling and heating systems switched off. Fig. 6 shows the TOP comparison between all combinations for the first floor during February. In general, the better behavior is with the C04 FF configurations and the worst with the C02 FF ones with single-layer brick and double-layer brick-tuff while, with single-layer tuff and double-layer tuff, the better behavior is described by C09 FF configurations and the worst by the C07 FF ones. Comparing the four graphs together, the lowest TOP value of 14.5 °C is reached by the combination C02 FF-B, while the higher TOP value of 18.5 °C is reached by C04 FF-B configuration, always in the case single-layer brick. It is important to note that the configuration with the lowest TOP oscillations is guarantee by the double-layer tuff.

In order to identify the configuration with the lowest TOP in summer (August), Fig. 7 shows the analysis for the first floor. The performances are inverted respect to the winter case, in particular, with single-layer brick and double-layer brick-tuff, the better behavior is described by C02 FF configurations and the worst by the C04 FF ones, while, with single-layer tuff and double-layer tuff, the better behavior is described by C07 FF and the worst by the C09 FF. It is interesting to note that the worst TOP trend of single-layer brick exceeds 42 °C, for double-layer brick-tuff exceeds 41 °C, for single-layer tuff is about 40 °C and exceeds 39 °C for double-layer tuff. About the better trend, for the single-layer brick and double-layer brick-tuff the minimum value is about 37 °C, while for the single-layer tuff is less than 37 °C and double-layer tuff reaches 36 °C. In general, for the summer month, the walls with tuff and tuff-tuff show the better behavior. Therefore, the double layer is preferred because it improves the response of the envelope in the summer regime.

The same analysis has been reproduced for the second floor, like shown in Fig. 8 for winter and Fig. 9 for summer. The TOP trends confirm the previous considerations for the first floor, but with some

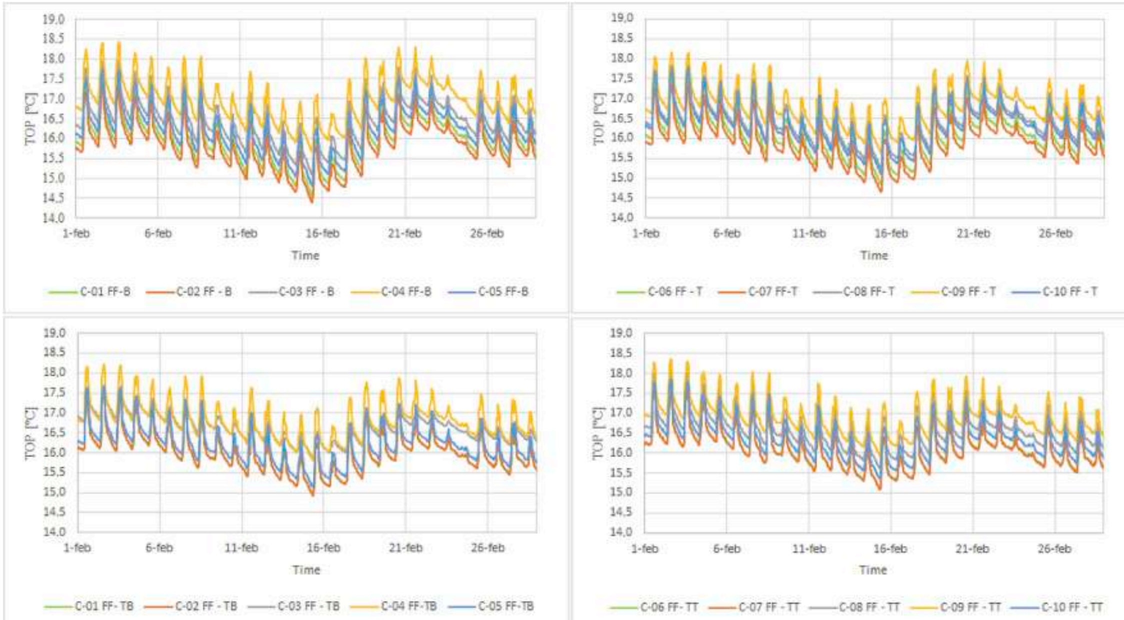

Fig. 6. TOP winter trend in February, first floor.

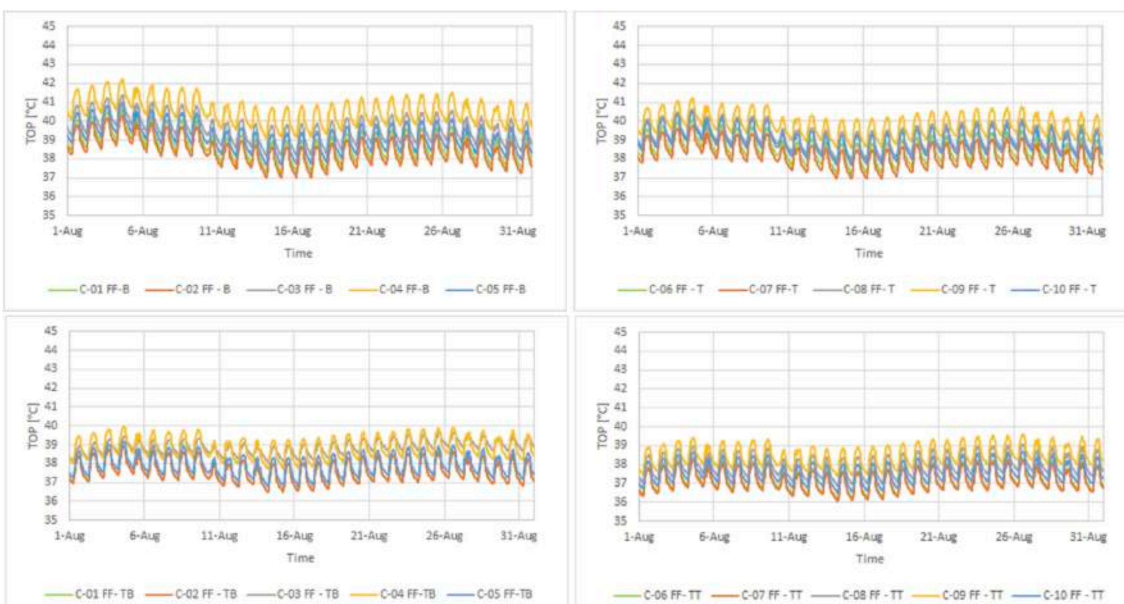

Fig. 7. TOP summer trend in August, first floor.

differences in the TOP ranges.

In winter, the TOP for the single-layer brick is between 15 °C and 18 °C, for the double-layer brick-tuff is between 15.5 °C and 17.5 °C, for single-layer tuff is about 16 °C and 18 °C, for double-layer tuff is 15.5 °C and 18 °C. Comparing with the same cases of the first floor, it is interesting to note that the ranges are reduced, the lowest and highest values are, respectively, improved and decreased of about 0.5 °C.

In summer, the lowest and highest peaks are 38.5 °C and 42.5 °C for the single-layer brick, 38 °C and 41 °C for the double-layer brick-tuff, 37.5 °C and 40.5 °C for the single-layer tuff, 37 °C and 39.5 °C for the double-layer tuff. It is interesting to note, from the comparison with the first floor (Fig. 7) that in general in the second floor the minimum peak is improved of about 1 °C and the maximum peak is decreased of 0.5 °C.

Table 7 shows the minimum, the average, the maximum and the standard deviation for each combination of the hottest season, for February and August.

The configurations highlighted with blue color are those with the best performances in the summer period, showing lowest values of average TOP, and medium behavior in the winter period.

The configurations with the orange color represent the best configurations in the winter period, showing the highest values of the average TOP, and a medium behavior in the summer period. The choice of the best configurations in the whole year depends on which period is predominant for the specific use of the building, summer or winter.

Fig. 10 shows the trend of the C-07 FF-TT and C-07 SF-TT after the addition of shading systems consisting of overhangs projecting on all windows as shown in Fig. 1. The addition of shading systems leads, during the winter period, to a bad decrease of TOP of about 0.18 °C

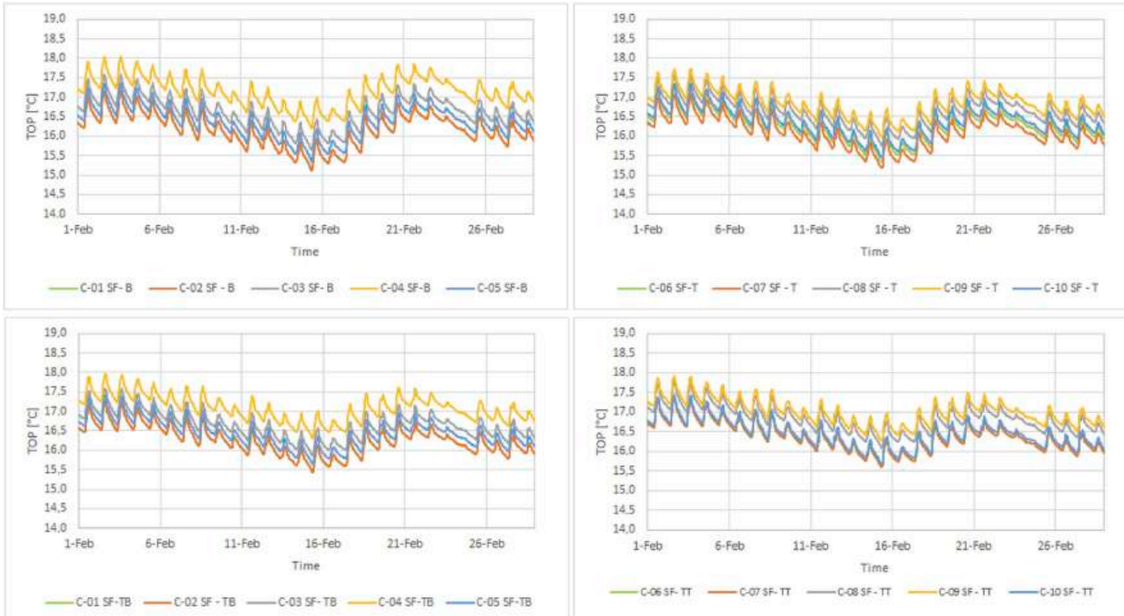

Fig. 8. TOP winter trend in February, second floor.

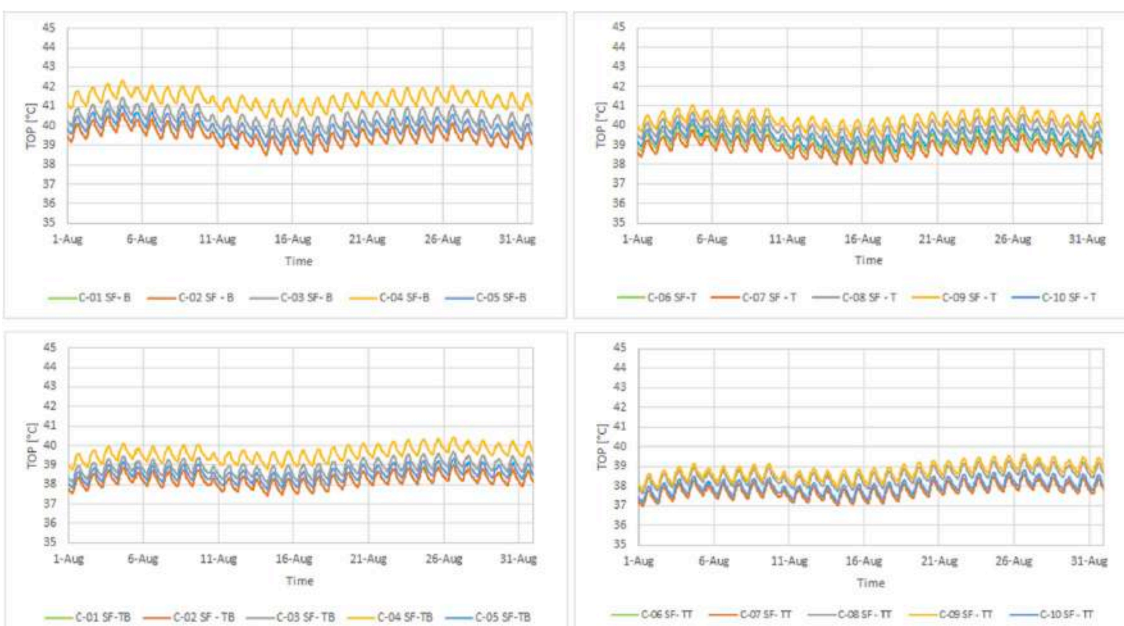

Fig. 9. TOP summer trend in August, second floor.

while, during the summer period, to a good decrease of TOP of about 1.81 °C. It suggests the installation of shading systems, especially in the Mediterranean climate.

Finally, the mechanical night ventilation has been switched on, during the summer season to improve the night-time cooling of the envelope. Fig. 11 shows the C-07 FF-TT with overhangs, considering three mechanical ventilation modes (1, 3 and 6 complete air changes for hour). The ventilation is turned on, during the summer period, from 20 p.m. to 6 a.m., during the rest of the day it is turned off. Respect to the no ventilation configuration C-07 FF-TT, the use of night-time cooling shows a drastically improvement of the performances, represented by values of TOP really lower. In details, if the ventilation with 6 Vol/h seems too much in term of human comfort because of high air velocities, the value of 3 Vol/h can be enough.

3.2. Analysis of different wall configurations

The wall performance changes according to various parameters, such as the thicknesses, positions and alternations of massive and insulation layers. Several wall configurations have been studied by varying such as parameters.

Fig. 12 shows how the TOP peak of the C-07 FF-TT changes varying the thickness of the massive layer (1-2-3) and the position of the insulation layer (4–5).

The C-07 FF-TT is characterized by the presence of two layers of 250 mm tuff and 100 mm of insulation (expanded cork panels) which is positioned outside (Combination 1 of the graph). It reaches the maximum operative air temperature of 38.2 °C.

Increasing the tuff thickness of 100 mm (Combination 2 of the

Table 7
Minimum, average, maximum and standard deviation of TOP in February and August.

COMBO	FEBRUARY				AUGUST			
	MIN	AVERAGE	MAX	ST. DEV.	MIN	AVERAGE	MAX	ST. DEV.
C-07 FF - TT	15.1	16.1	17.6	0.5	36.1	37.2	38.2	0.5
C-06 FF- TT	15.1	16.1	17.7	0.5	36.2	37.3	38.4	0.5
C-10 FF - TT	15.3	16.4	17.9	0.5	36.5	37.6	38.7	0.5
C-01 FF- TB	14.9	16	17.5	0.5	36.5	37.6	38.9	0.5
C-02 FF - TB	14.9	16	17.5	0.5	36.5	37.6	38.9	0.5
C-06 SF- TT	15.6	16.4	17.4	0.4	37	37.8	38.6	0.3
C-07 SF- TT	15.6	16.4	17.4	0.4	37	37.8	38.6	0.3
C-05 FF-TB	15.1	16.2	17.7	0.5	36.8	37.9	39.2	0.5
C-08 FF - TT	15.6	16.6	18.1	0.5	36.9	38	39.1	0.5
C-10 SF - TT	15.7	16.5	17.4	0.4	37.2	38	38.8	0.3
C-01 SF-TB	15.4	16.3	17.3	0.4	37.4	38.2	39	0.3
C-02 SF - TB	15.5	16.3	17.3	0.4	37.4	38.2	39	0.3
C-07 FF-T	14.7	15.9	17.4	0.5	36.9	38.2	39.8	0.6
C-09 FF - TT	15.9	16.9	18.3	0.4	37.4	38.5	39.6	0.5
C-08 SF - TT	16.1	16.8	17.8	0.3	37.6	38.5	39.4	0.4
C-06 FF - T	14.8	16.1	17.6	0.5	37.2	38.5	40.1	0.6
C-02 FF - B	14.4	15.8	17.3	0.6	37	38.5	40.3	0.7
C-05 SF-TB	15.6	16.5	17.4	0.4	37.7	38.6	39.3	0.3
C-09 SF - TT	16.3	17	17.9	0.3	37.8	38.7	39.6	0.4
C-04 FF-TB	15.8	16.8	18.2	0.5	37.7	38.8	40	0.5
C-01 FF-B	14.6	16	17.5	0.6	37.3	38.8	40.7	0.7
C-03 FF - TB	15.9	16.7	17.6	0.3	38.1	38.9	39.7	0.3
C-03 SF- TB	15.9	16.7	17.6	0.3	38.1	38.9	39.7	0.3
C-07 SF - T	15.2	16.1	17.1	0.4	38	38.9	39.8	0.4
C-10 FF - T	15.1	16.3	17.8	0.5	37.7	39	40.5	0.6
C-05 FF-B	14.8	16.2	17.7	0.6	37.7	39.1	41	0.7
C-08 FF- T	15.3	16.4	17.8	0.5	37.9	39.2	40.6	0.6
C-06 SF-T	15.3	16.3	17.3	0.4	38.3	39.2	40.1	0.4
C-10 SF - T	15.5	16.4	17.4	0.4	38.5	39.4	40.3	0.4
C-01 SF- B	15.1	16.2	17.2	0.4	38.5	39.5	40.6	0.4
C-02 SF - B	15.1	16.2	17.2	0.4	38.5	39.5	40.6	0.4
C-04 SF-TB	16.3	17.1	18	0.3	38.8	39.6	40.4	0.4
C-03 FF - B	15.1	16.5	17.9	0.6	38.1	39.6	41.4	0.7
C-09 FF - T	15.7	16.8	18.2	0.5	38.6	39.8	41.2	0.6
C-08 SF - T	15.8	16.7	17.6	0.4	39	39.9	40.7	0.3
C-05 SF-B	15.4	16.4	17.4	0.4	38.9	39.9	41	0.4
C-09 SF - T	16	16.8	17.7	0.4	39.4	40.3	41	0.3
C-03 SF- B	15.6	16.6	17.6	0.4	39.4	40.4	41.4	0.4
C-04 FF-B	15.7	17	18.4	0.5	39.1	40.5	42.3	0.7
C-04 SF-B	16.2	17.1	18.1	0.4	40.4	41.4	42.3	0.4

graph), the maximum operative air temperature decreases by 1 °C, reaching 37.15 °C.

If the tuff thickness is further increased by 100 mm (Combination 3 of the graph), the maximum operative air temperature decreases by 1 °C, reaching 36.04 °C. Combination 3 represents the combination with two layers of tuff of 450 mm, 100 mm of insulation placed outside.

Combination 4 represents the combination with two layers of tuff of 450 mm, 100 mm of insulation positioned between the two layers of tuff, the TOP is 37.49 °C. Compared to Combination 3 the TOP increases by 1 °C.

Combination 5 represents the combination with two layers of tuff of 450 mm, 100 mm of insulation placed inside. The operative air temperature is 40.25 °C. Compared to combination 3, the operative air temperature increases by 4 °C.

The study conducted by Jie Deng et al [51] applies the state-space method validated by the simulation results from EnergyPlus. The results confirm that walls characterized by high level of mass on the internal side lead to a major control of the internal thermal comfort and it is preferable to place the insulation layer on the external side to avoid overheating problems.

3.3. Useful thermal requirement

To complete the analysis the energy performance indexes, expressed in kWh/m^{2}year, have been carried out.

Table 8 shows values of $EP_{H,nd}$ and $EP_{C,nd}$ for all combinations, that represent the thermal performance indices useful for heating and cooling, respectively. These values are relating to the envelope given by the ratio between the useful heat energy requirement and the usable area. They must be lower than the corresponding limit value calculated for the reference building $EP_{H,\ nd,rif}$ and $EP_{C,\ nd,rif}$). The term "reference building" indicates a building identical to the analyzed one in terms of: geometry (shape, volumes, floor area, surfaces of construction elements and components), orientation, location, intended use, boundary conditions. The reference building is characterized by predetermined thermal characteristics and energy parameters in accordance with Appendix A of Annex 1 of Ministerial Decree 26/6/15 [52].

4. Conclusions

Buildings located in warm climates are affected by serious overheating problems, for most of the year.

This paper has shown the application of a methodology to identify the optimal design of the building envelope, to avoid overheating problems without the use of cooling systems.

The proposed method is based on a comparative evaluation of several external wall configurations, by monitoring the internal operative temperature of a low-rise residential buildings in warm Mediterranean climate. The choice of the wall configurations has been done between the most used building materials in the Italian context.

The software Termolog Epix 9 has been used for the calculation of the hourly energy performance of the building, by the Dynamic

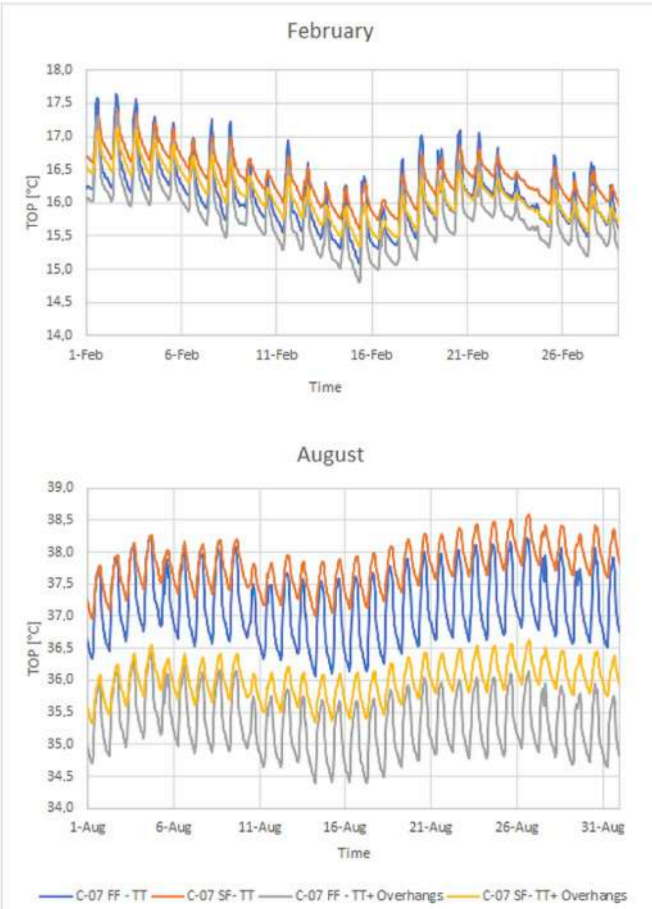

Fig. 10. TOP of C-07 FF-TT and C-07 SF-TT with and without overhangs.

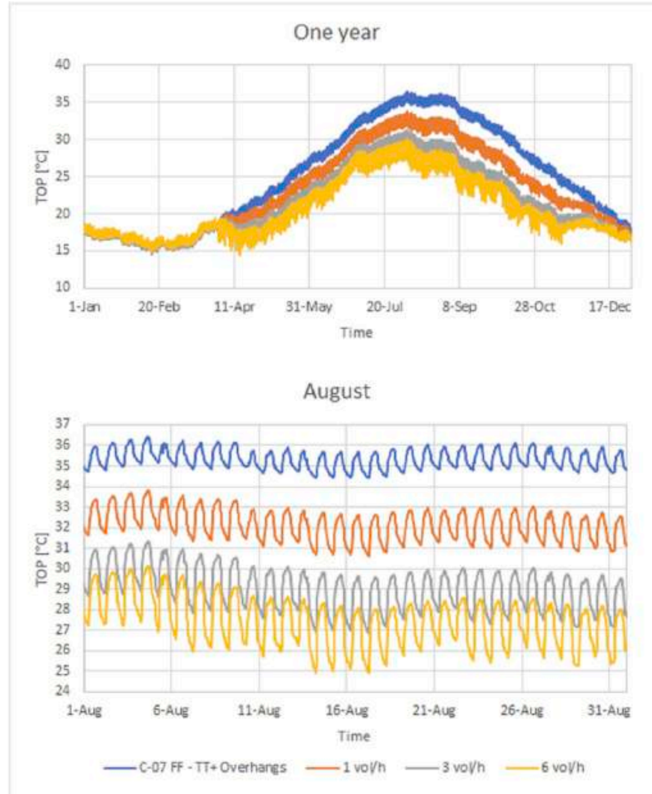

Fig. 11. TOP of C-07 FF-TT with overhangs and three mechanical ventilation modes.

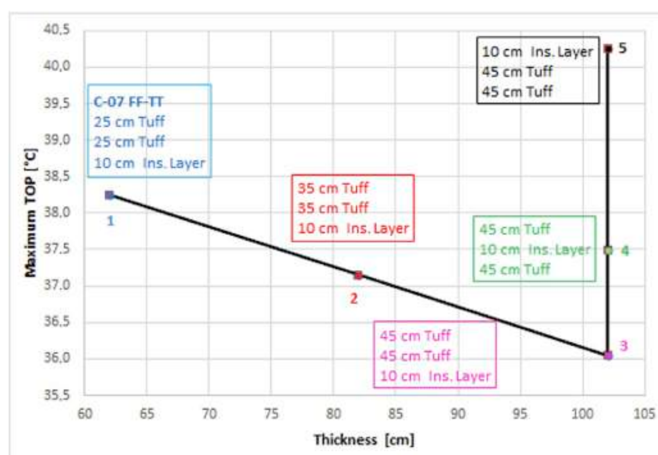

Fig. 12. TOP peaks of C-07 FF-TT (1) changing the massive layer thickness (2–3) and the position of insulation layer (4–5).

Calculation Engine. The algorithms are based on the hourly method proposed by the UNI EN ISO 52016. The hourly method allows the assessment of the internal temperature of a thermal zone by resolution, in a transitory regime on an hourly basis, of a system of equations which describe the thermal exchanges which occur between internal and external environment through the envelope.

The results underline that the best solutions are characterized by the presence of walls composed by double layer of tuff, with a very massive layer in the internal side and resistive layer outside. It ensures a comfortable indoor environment by attenuating TOP oscillations. In particular, the configurations C-07 FF-TT and C-07 SF-TT, with double layer of tuff and expanded cork panel, are those with the best performances in the summer period, showing lowest values of average TOP, and medium behavior in the winter period.

Improving the thickness of the massive layers the TOP peaks in summer season strongly decreases, but it can be not economically convenient. In summer, between all solutions, the best one is with the insulation layer placed on the external side.

Once optimized the envelope, this study suggests the addition of shading systems consisting of overhangs projecting on all windows. The building characterized by walls with double layer of tuff (C-07 FF-TT and C-07 SF-TT) reaches a bad decrease of TOP of about 0.18 °C in winter and a good decrease of TOP of about 1.81 °C in summer. This further improvement during the hot season suggests the installation of shielding systems, particularly in the Mediterranean climate.

At the end, this study demonstrates that, once optimized the envelope, it is easier to reach good values of operative temperature with the only use of a mechanical ventilation system.

This methodology can be a valid support for technicians in the identification of the best solutions to achieve highly efficient and comfortable buildings.

Once optimized the building envelope, future developments are the application of a horizontal earth-to-air heat exchanger to air conditioning the internal environment, considering also different building uses.

Furthermore, the cost optimal analysis can represent a valid support in the final choice of the best solution, from a technical and economic point of view.

Author contributions

Work plan, P.M.C.; Simulations, C.B., G.C; Analysis of result: C.B., G.

Table 8
$EP_{h,nd}$ and $EP_{c,nd}$ for real and reference buildings.

	Real building		Reference building	
	EPH, nd	EPC, nd	EPH, nd,rif	EPC, nd,rif
	(kWh/m^2)	(kWh/m^2)	(kWh/m^2)	(kWh/m^2)
C-01 B	17.9	18.6	23.1	19.8
C-01 TB	18.7	18.0	25.3	18.3
C-02 B	18.3	18.0	23.5	19.2
C-02 TB	19.1	17.3	25.3	18.3
C-03 B	16.0	19.0	23.0	19.8
C-03 TB	17.3	17.7	25.3	18.3
C-04 B	14.2	19.5	23.0	19.8
C-04 TB	15.5	18.1	25.3	18.3
C-05 B	17.0	18.8	23.0	19.8
C-05 TB	18.3	17.5	25.3	18.3
C-06 T	18.0	18.5	23.1	19.8
C-06 TT	19.3	17.2	25.5	18.2
C-07 T	18.9	17.4	24.0	18.5
C-07 TT	18.9	17.6	25.4	18.2
C-08 T	16.0	18.6	24.0	19.0
C-08 TT	16.8	18.4	25.5	18.9
C-09 T	15.0	18.9	24.4	19.8
C-09 TT	15.8	18.7	25.9	19.0
C-10 T	16.8	19.4	23.6	19.6
C-10 TT	18.2	18.1	26.0	18.1

C. and P.M.C.; Writing: C.B.; Revision of the manuscript: P.M.C.

Declaration of competing interest

The authors declare no conflict of interest.

Nomenclature

c	Specific heat capacity (J/kgK)
d	Thickness of a layer (m)
Δt	Time Shift (h)
E	Energy performance index
$E_{pc,n}$	Thermal performance index useful for cooling (kWh/m^2)
$E_{ph,n}$	Thermal performance index useful for heating (kWh/m^2)
fd	Decrement Factor
hc	Convective Heat Transfer Coefficient
hr	Linear Radiative Heat Transfer Coefficient
$\square_1$	Internal Thermal Capacity (kJ/m^{2}K)
K_2	External Thermal Capacity (kJ/m^{2}K)
Ms	Total Surface Mass (Kg/m^2)
PMN	Average Expected Score
PPD	Expected Percentage of Dissatisfied
R	Thermal Resistance (m^{2}K/W)
S/V	Shape Factor
T	Period of the variations (s)
T_{db}	Air Temperature (dry bulb temperature) (°C)
T_{mr}	Mean Radiant Temperature (°C)
TOP	Operative Air Temperature (°C)
U	Thermal Transmittance under steady state boundary conditions (W/m^{2}K)
Y_{11}	Internal Admittance (W/m^{2}K)
Y_{12}	Periodic Thermal Transmittance (W/m^{2}K)
Y_{22}	External Thermal Admittance (W/m^{2}K)

Greek letters

l	design thermal conductivity (W/mK)
r	density (kg/m^3)

Subscripts

m,n	for the thermal zones
a	air layer
1	internal
2	external
mr	mean radiant
r	radiative
db	dry bulb
ph,nd	index useful for heating
pc,nd	index useful for cooling

Appendix A. Supplementary data

Supplementary data to this article can be found online at https://doi.org/10.1016/j.jobe.2019.101059.

References

[1] EPBD recast, Directive (EU) 2018/844 of the European Parliament and of the Council of 30 May 2018 amending Directive 2010/31/EU on the energy performance of buildings and Directive 2012/27/EU on energy efficiency (Text with EEA relevance)PE/4/2018/REV/1OJ L 156, Off.J.Eur. Union (2018) 75–91. http://data.europa.eu/eli/dir/2018/844/oj.

[2] C. Baglivo, P.M. Congedo, D. D'Agostino, I. Zacà, Cost-optimal analysis and technical comparison between standard and high efficient mono-residential buildings in a warm climate, Energy 83 (2015) 560–575.

[3] I. Zacà, D. D'Agostino, P.M. Congedo, C. Baglivo, Data of cost-optimality and technical solutions for high energy performance buildings in warm climate, Data Brief 4 (2015) 222–225.

[4] P. Valdiserri, C. Biserni, Energy performance of an existing office building in the northern part of Italy: retrofitting actions and economic assessment, Sustain. Cities Soc. 27 (2016) 65–72.

[5] D. Castro-Lacouture, J.A. Sefair, L. Flórez, A.L. Medaglia, Optimization model for the selection of materials using a LEED-based greenbuilding rating system in Colombia, Build. Environ. 44 (2009) 1162–1170.

[6] F. Stazi, F. Naspi, G. Ulpiani, C. Di Perna, Indoor air quality and thermal comfort optimization in classrooms developing an automatic system for windows opening and closing, Energy Build. (2017) 732–746.

[7] M. Arif, M. Katafygiotou, A. Mazroei, A. Kaushik, E. Elsarrag, Impact of indoor environmental quality on occupant well-being and comfort: a review of the literature, Int. J. Sustain. Built Environ. 5 (2016) 1–11.

[8] J. García-Sanz-Calcedo, M. Gómez-Chaparro, Quantitative analysis of the impact of maintenance management on the energy consumption of a hospital in Extremadura (Spain), Sustainable Cities and Society 30 (2017) 217–222, https://doi.org/10.1016/j.scs.2017.01.019. ISSN 2210-6707.

[9] Farheen Bano, Vandana Sehgal, Evaluation of energy-efficient design strategies: comparison of the thermal performance of energy-efficient office buildings in composite climate, India, Sol. Energy 176 (2018) 506–519, https://doi.org/10.1016/j.solener.2018.10.057. ISSN 0038-092X.

[10] H. Yoshino, T. Hong, N. Nord, IEA EBC Annex 53: Total Energy Use in Buildings—Analysis and Evaluation Methods, Bruna Faitão Balvedi, Enedir Ghisi, (Roberto Lamberts).

[11] Bertug Ozarisoy, Assessing overheating risk and thermal comfort in state-of-the-art prototype houses that combat exacerbated climate change in UK, Energy Build. 187 (2019) 201–217, https://doi.org/10.1016/j.enbuild.2019.01.030. ISSN 0378-7788.

[12] I. Zacà, D. D'Agostino, P.M. Congedo, C. Baglivo, Assessment of cost-optimality and technical solutions in high performance multi-residential buildings in the Mediterranean area, Energy Build. 102 (2015) 250–265.

[13] Cristina Baglivo, Paolo Maria Congedo, Matteo Di Cataldo, Luigi Damiano Coluccia, Delia D'Agostino, Envelope design optimization by thermal modeling of a building in a warm climate, Energies 10 (2017) 1808, https://doi.org/10.3390/en10111808.

[14] P.M. Congedo, C. Baglivo, I. Zacà, High performance solutions and data for nzebs offices located in warm climates, Data Brief 5 (2015) 502–505.

[15] Chengcheng Xu, Shuhong Li, Kaikai Zou, Study of heat and moisture transfer in internal and external wall insulation configurations, J Build Eng (2019) 2352–7102, https://doi.org/10.1016/j.jobe.2019.02.016. ISSN.

[16] Fei Cheng, Xu Zhang, Xing Su, Comparative assessment of external and internal insulation for intermittent air-conditioned bedrooms in Shanghai, Procedia Engineering 205 (2017) 50–55, https://doi.org/10.1016/j.proeng.2017.09.933. ISSN 1877-7058.

[17] M. Kolokotroni, A. Aronis, Cooling-energy reduction in air-conditioned offices by using night ventilation, Appl. Energy 63 (4) (1999) 241–253.

[18] T. Kubota, D. Chyee, S. Ahmad, The effects of night ventilation technique on indoor thermal environment for residential buildings in hot-humid climate of Malaysia, Energy Build. 41 (8) (2009) 829–839.

[19] E. Shaviv, A. Yezioro, I. Capeluto, Thermal mass and night ventilation as passive cooling design strategy, Renew. Energy 24 (no. 3–4) (2001) 445–452.

[20] B. Givoni, Climate Considerations in Building and Urban Design, Lo Van Nostrand Reinhold, New York, 1998.

[21] A. Michael, D. Demosthenous, M. Philokyprou, Natural Ventilation for cooling in Mediterranean climate: a case study in vernacular architecture of Cyprus, Energy Build. 144 (2017) 333–345.

[22] Ö.A. Dombaycı, M. Gölcü, Y. Pancar, Optimization of insulation thickness for external walls using different energy-sources, Appl. Energy 83 (2006) 921–928.
[23] P. Valdiserri, C. Biserni, M. Garai, Energy performance of a ventilation system for an apartment according to the Italian regulation, Int. J. Energy Environ. Eng. 7 (2016) 353–359.
[24] Fatima Harkouss, Fardoun Farouk, Pascal Henry Biwole, Passive design optimization of low energy buildings in different climates, Energy 165 (Part A) (2018) 591–613, https://doi.org/10.1016/j.energy.2018.09.019. ISSN 0360-5442.
[25] M. Kottek, J. Grieser, C. Beck, B. Rudolf, F. RubelWorld, Map of the Köppen-Geiger climate classification updated Meteorol Z 15 (2006) 259–263, https://doi.org/10.1127/0941-2948/2006/0130.
[26] Cristina Baglivo, Paolo Maria Congedo, High performance precast external walls for cold climate by a multi-criteria methodology, Energy 115 (Part 1) (2016) 561–576, https://doi.org/10.1016/j.energy.2016.09.018. ISSN 0360-5442.
[27] Cristina Baglivo, Paolo Maria Congedo, Andrea Fazio, Domenico Laforgia, Multi-objective optimization analysis for high efficiency external walls of zero energy buildings (ZEB) in the Mediterranean climate, Energy Build. 84 (2014) 483–492, https://doi.org/10.1016/j.enbuild.2014.08.043. ISSN 0378-7788.
[28] A. Sarkar, S. Bose, Exploring impact of opaque building envelope components on thermal and energy performance of houses in lower western Himalayans for optimal selection, J. Build. Eng. 7 (2016) 170–182.
[29] Sami A. Al-Sanea, M.F. Zedan, S.N. Al-Hussain, Effect of thermal mass on performance of insulated building walls and the concept of energy savings potential, Appl. Energy 89 (Issue 1) (January 2012) 430–442, https://doi.org/10.1016/j.apenergy.2011.08.009. ISSN 0306-2619.
[30] N. Cardinale, G. Rospi, P. Stefanizzi, Energy and microclimatic performance of Mediterranean vernacular buildings: the Sassi district of Matera and the Trulli district of Alberobello, Build. Environ. 59 (2013) 590–598.
[31] E. Minne, K. Wingrove, J.C. Crittenden, Influence of climate on the environmental and economic life cycle assessments of window options in the United States, Energy Build. 102 (2015) 293–306.
[32] J. Xamán, C. Pérez-Nucamendi, J. Arce, J. Hinojosa, G. Álvarez, I. Zavala-Guillén, Thermal analysis for a double pane window with a solar control film for using in cold and warm climates, Energy Build. 76 (2014) 429–439.
[33] P.O. Fanger, A.K. Melikov, H. Hanzawa, J. Ring, Turbulence and draft, ASHRAE J. 31 (1989) 18–23.
[34] P.O. Fanger, Thermal Comfort, Analysis and Application in Environmental Engineering, Mcgraw-Hill, New York, NY, USA, 1972.
[35] A. Pourshaghaghy, M. Omidvari, Examination of thermal comfort in a hospital using PMV–PPD model, Appl. Ergon. 43 (2012) 1089–1095.
[36] ISO 7730, Ergonomics of the Thermal Environment—Analytical Determination and Interpretation of Thermal Comfort Using Calculation of the PMV and PPD Indices and Local Thermal Comfort, International Standardization Organization, Geneva, Switzerland, 2005.
[37] J. Andersson, A. Boerstra, D. Clements-Croome, K. Fitzner, S.O. Hanssen, Indoor Climates and Productivity in Offices, REHVA (Federation of European Heating, Ventilation and Air Conditioning Associations), Brussels, Belgium, 2006.
[38] D. D'Agostino, P.M. Congedo, CFD modeling and moisture dynamics implications of ventilation scenarios in historical buildings, Build. Environ. 79 (2014) 181–193.
[39] S. Kephalopoulos, O. Geiss, J. Barrero-Moreno, D. D'Agostino, D. Paci, Promoting Healthy and Energy Efficient Buildings in the European Union—National Implementation of Related Requirements of the Energy Performance Buildings Directive (2010/31/EU), European Commission's Science and Knowledge Service, Brussels, Belgium, 2016.
[40] O. Seppänen, W.J. Fisk, D. Faulkner, Cost benefit analysis of the night-time ventilative cooling, in: Proceedings of the 7th International Conference on Healthy Buildings, vol. 3, 2003, pp. 394–397. Singapore, 7–11 December 2003.
[41] A. Hasan, M. Vuolle, K. Sirén, Minimisation of life cycle cost of a detached house using combined simulation and optimization, Build. Environ. 43 (2008) 2022–2034.
[42] UNI 10375:2011, Calculation method of the indoor temperature of a room in the warm period, Available online: https://infostore.saiglobal.com/store/details.aspx?ProductID=1497581, , 2011. (Accessed 8 October 2017).
[43] Istat, Census on Population, Statistics by the National Institute of Statistics, 2012 available at: http://dati-censimentopopolazione.istat.it.
[44] J. Salazar, 21 - life cycle assessment (LCA) of windows and window materials, in: F. Pacheco-Torgal, L.F. Cabeza, J. Labrincha, A. de Magalhães (Eds.), Eco-Efficient Construction and Building Materials, Woodhead Publishing, 2014, ISBN 9780857097675, pp. 502–527, https://doi.org/10.1533/9780857097729.3.502.
[45] K. Tsikaloudaki, Th Theodosiou, K. Laskos, D. Bikas, Assessing cooling energy performance of windows for residential buildings in the Mediterranean zone, Energy Convers. Manag. 64 (December 2012) 335–343, https://doi.org/10.1016/j.enconman.2012.04.020. ISSN 0196-8904.
[46] UNI EN ISO 13786, Thermal Performance of Building Components - Dynamic Thermal Characteristics - Calculation Methods, 2018. ISO 13786:2017.
[47] European norm EN ISO 13788, Hygrothermal performance of building components and building elements, Internal surface temperature to avoid critical surface humidity and interstitial condensation, Calculation methods (2013).
[48] Lamberto Tronchin, Kristian Fabbri, Energy Performance Certificate of building and confidence interval in assessment: an Italian case study, Energy Policy 48 (2012) 176–184, https://doi.org/10.1016/j.enpol.2012.05.011. ISSN 0301-4215.
[49] ISO 52016, Energy Performance of Buildings—Energy Needs for Heating and Cooling, Internal Temperatures and Sensible and Latent Heat Loads —Part 1: Calculation Procedures, 2017.
[50] ANSI/ASHRAE55 Standard, Thermal Environmental Conditions for Human Occupancy ASHRAE, 2013. Atlanta.
[51] Jie Deng, Runming Yao, Wei Yu, Qiulei Zhang, Baizhan Li, Effectiveness of the thermal mass of external walls on residential buildings for part-time part-space heating and cooling using the state-space method, Energy Build. 190 (2019) 155–171, https://doi.org/10.1016/j.enbuild.2019.02.029. ISSN 0378-7788.
[52] Ministry of Economic Development (Italy), Inter-Ministerial Decree 26 June 2015 - Adaptation of National Guidelines for Energy Certification of Buildings, June 2015.